iForest
Biogeosciences and Forestry

Research Article
doi: 10.3832/ifor1744-009
vol. 10, pp. 259-266

High resolution biomass mapping in tropical forests with LiDAR-derived Digital Models: Poás Volcano National Park (Costa Rica)

Alfredo Fernández-Landa [(1)],
José Antonio Navarro [(1-2)],
Sonia Condés [(2)],
Nur Algeet-Abarquero [(1-3)],
Miguel Marchamalo [(3)]

Tropical forests play a key role in global carbon cycle. Reducing Emissions from Deforestation and forest Degradation (REDD+) program requires reliable mechanisms for Monitoring, Reporting and Verification (MRV). In this regard, new methods must be developed using updated technologies to assess carbon stocks. The combination of LiDAR technology and *in situ* forest networks allows the estimation of biomass with high resolution in low data environments, such as tropical countries. However, the evaluation of current LiDAR methods of biomass inventory, and the development of new methodologies to reduce uncertainty and increase accuracy, is still needed. Our aim is to evaluate new methodologies of spatially explicit LiDAR biomass inventories based on local and general plot-aggregate allometry. For this purpose, 25 field plots were inventoried, covering the structural and ecological variability of Poás Volcano National Park (Costa Rica). Important differences were detected in the estimation of aboveground biomass (92.74 t ha^{-1} considering the mean value of plot sample) depending on the chosen tree allometry. We validated the general aboveground biomass plot-aggregate allometry proposed by Asner & Mascaro (2014) in our study area, and we fitted two specific models for Poás forests. Both locals and general models depend on LiDAR top-of-canopy height (TCH), basal area (BA) and wood density. Small deviations in the wood density plot sample (0.60 ± 0.05) indicated that a single wood density constant value could be used throughout the study area. A BA-TCH origin forced linear model was fitted to estimate basal area, as suggested by the general methodology. Poás forest has a larger biomass density for the same THC compared to the rest of the forests previously studied, and shows that the BA-TCH relationship might have different trends in each life zone. Our results confirm that the general plot-aggregate methodology can be easily and reliably applied as aboveground biomass in a new area could be estimated by only measuring BA in field plots to obtain a local BA-TCH regression. For both local and general methods, the estimation of BA is critical. Therefore, the definition of precise basal area field measurement procedures is decisive to achieve reliable results in future studies.

Keywords: Carbon, Remote Sensing, REDD, LiDAR, Plot-level Allometry, Biomass, Basal Area

Introduction

The Fourth Assessment Report of the Intergovernmental Panel on Climate Change (IPCC 2005) reports an increment in the global average temperature related to an increase of 70% in Greenhouse Gas (GHG) emissions due to human activities since 1970 (IPCC 2007). Forests play a double role of particular importance on adjustment of the global carbon cycle, acting as both carbon emission sources and sinks. Emissions due to deforestation, degradation of the forests and land use changes encompass 17.3% of total GHG emissions (IPCC 2007). As carbon pools, the IPCC (2007) estimates that forests contain 77% of carbon stored in global forest vegetation and 39% of carbon in soils. In this regard, tropical forests are very important as they can store more carbon per hectare than other forests (Houghton 2005), with estimates in the order of 25% of carbon in the biosphere (Bonan 2008). According to the FAO Forest Resources Assessments 2010 (Simonian et al. 2010), the highest deforestation rates can be found in the tropics, hence tropical forests are the most threatened ecosystems on earth.

In order to curb the GHG emissions due to forest losses, Reducing Emissions from Deforestation and forest Degradation (REDD+) scheme was recognized as a valid mechanism against climate change in the

(1) Agresta Soc. Coop, C/ Duque de Fernán Núñez 2, Madrid 28012 (Spain); (2) Dept. Natural Systems and Resources, Technical University of Madrid. School of Forestry, Ciudad Universitaria, Madrid 28040 (Spain); (3) Dept. of Land Morphology and Engineering, Technical University of Madrid, Ciudad Universitaria, Madrid 28040 (Spain)

@ Alfredo Fernández-Landa (afernandez@agresta.org)

Received: Jun 18, 2015 - Accepted: Oct 20, 2016

Citation: Fernández-Landa A, Navarro JA, Condés S, Algeet-Abarquero N, Marchamalo M (2017). High resolution biomass mapping in tropical forests with LiDAR-derived Digital Models: Poás Volcano National Park (Costa Rica). iForest 10: 259-266. – doi: 10.3832/ifor1744-009 [online 2017-02-23]

Communicated by: Davide Travaglini

2010 Cancun Agreement (UNFCCC COP-16 Conference). Costa Rica joined this initiative integrating the carbon captured data from its National Parks and Biological Reserves into the schemes framework, which consequently became one of the main points in its REDD+ strategy approved in 2008.

A transparent system for Monitoring, Reporting and Verification (MRV) is a necessary requirement of REDD+ activity. If accurate estimates of carbon are expected then this process could prove costly; hence, it is important to develop efficient methods to carry out large-scale precise and inexpensive measurements. Wall-to-wall high resolution estimations of biomass and carbon stocks in tropical areas are crucial to quantify emissions from forest loss, gain and growth, but also to identify, describe, and quantify emissions from forest degradation. Quantifying emissions from forest degradation in tropical forests is a major concern as forest degradation might represent a significant percentage of nationwide emissions of greenhouse gases (Murdiyarso et al. 2008). Some authors pointed out that those emissions from forest degradation can be of the same magnitude as those caused by deforestation (Sasaki & Putz 2009). Wall-to-wall mapping can lead to a better understanding of land use dynamics and an easier identification of drivers of forest degradation and deforestation. Therefore, the incorporation of these methods could lead to a substantial improvement in forest management, supporting the formulation of environmental policies, planning tools and actions to improve the status and conservation of forests.

Light Detection and Ranging (LiDAR) is an active remote sensing technique based on a laser sensor. It is a powerful technology for accurate estimates of the spatial variability in forest carbon stocks. Although LiDAR data acquisition may be expensive (Gibbs et al. 2007, Pirotti 2011), it is the most appropriate technology at scales ranging from one to several million hectares and is useful for calibrating broader-scale Interferometric Synthetic Aperture Radar measurements (Sexton et al. 2009). Other authors (Mitchard et al. 2012) showed that space-based LiDAR, such as the Geoscience Laser Altimeter System, might be useful as a resource to assist the mapping of forest biomass carbon stocks using the classification of high resolution optical rather than radar data.

The effectiveness of LiDAR technology to estimate forest variables in tropical forest has been proved in different works. Clark et al. (2004) estimated mean tree height for plantation plots at La Selva Biological Station (Costa Rica) using plot mean LiDAR height with a model R^2 of 0.97 and 1.08 m of root-mean-square error (RMSE). Clark et al. (2011), also working in La Selva forest, obtained an aboveground biomass model with an R^2 of 0.90 and RMSE of 38.3 Mg ha^{-1} including in the model two LiDAR metrics (plot-level mean height and maximum height).

Asner et al. (2012a) used the vertical center of canopy volumetric profile, also known as mean canopy profile height (MCH) to fit regional and universal models. These authors were able to predict aboveground carbon density in different tropical locations using a single universal LiDAR model (R^2 = 0.80, RMSE = 27.6 Mg C ha^{-1}). Although this approach showed to be consistent when using a single LiDAR sensor (Asner et al. 2012a), an approach based on the variable top-of-canopy height (TCH) has proved to be more consistent across different sensor characteristics (Asner & Mascaro 2014). Therefore, the latter authors developed a general plot-aggregate allometry based on the TCH variable using a LiDAR plot network of tropical forest sites in Colombia, Hawaii, Madagascar, Peru and Panama to evaluate carbon density across a wide range of tropical vegetation conditions. TCH is derived from the LiDAR digital canopy model and is a consistent index among different modern LiDAR sensors (Asner & Mascaro 2014). According to them, this general methodology can largely reduce fieldwork for LiDAR inventories in tropical areas because aboveground biomass could be estimated by only measuring basal area in field plots to obtain regional basal area-TCH regression.

The aim of this paper is to validate the general aboveground biomass (AGB) plot-aggregate equation developed by Asner & Mascaro (2014) in Poás forest (Costa Rica) and to compare the results found through this model to those obtained through local models fitted for the study area. The main objective was to assess the validity of this general model and the advantages of fitting local models instead of using the Asner & Mascaro's equations. Poás Volcano National Park is an appropriate area to test this AGB plot-aggregate approach due to the large structural and ecological variability in the area. Furthermore, to evaluate the importance of the tree allometry in wall-to-wall AGB estimations, two general individual tree allometric biomass equations proposed by Chave et al. (2005) have been used.

Material and methods

Study area and input data

The study was carried out in the Poás Volcano National Park (6506 ha), in the province of Alajuela (Costa Rica – Fig. 1). It is a stratovolcano complex with a generally steep terrain ranging from 1099 to 2713 m in elevation, with a mean annual precipitation and temperature gradient of approximately 2300-5100 mm y^{-1} and 9-15 °C, respectively. Due to the existence of two slopes (Atlantic and Pacific slopes), an abrupt topography and a wide altitude range is observed, with significant fluctuations in mean annual precipitation and temperature throughout the study area.

According to the ecological map of Costa Rica (Bolaños et al. 2005). Poás Volcano area hosts forests corresponding to Holdridge's life zones of montane rainforest (M-RF), lower montane rainforest (LM-RF), montane transition to lower montane rainforest (M-LM), premontane rainforest (PM-RF) and lower montane wet forest (LM-WF – Fig. 1).

Input data was a 1-m resolution Digital Elevation Model (DEM) and a Digital Surface Model (DSM) generated from an airborne LiDAR flight executed by Stereocarto S.L. in July 2010. The area was surveyed with the ALS50-II-MpiA sensor (multi pulse in air) achieving a mean point density of 1 point m^{-2}. These data were projected in the CR05 Reference System and the Transversal Mercator projection for Costa Rica CRTM05. A Digital Canopy Model (DCM) that represents the maximum vegetation height in each 1-m pixel was obtained from the subtraction of the DEM and the DSM.

In order to encompass the range of struc-

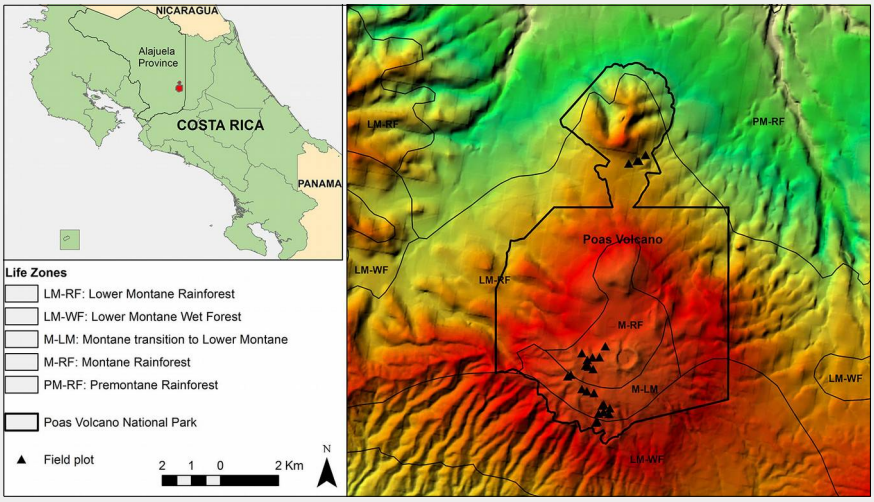

Fig. 1 - Location of Poás Volcano National Park in Alajuela Province (Costa Rica) and spatial distribution of field plots and Holdrige's life zones in the area.

tural and ecological variability in the Park, a stratified sample throughout the different life zones of Holdridge was conducted. For this, we generated LiDAR-derived canopy height maps to identify the vertical and horizontal structural differences in the forest. Thus, a 20 m resolution raster was built from a three statistics code. The three parameters measured in each 20×20 pixel were: (i) canopy cover as percentage of 0×1 m pixels above 2.00 m; (ii) 95th height percentile (P95); and (iii) interquartile range (IQ). They were codified in class values taking into account each parameter range (Tab. 1)

Field plot estimation

Transects were designed following the roads and trails within the study area and a total of 25 circular sampling plots of 0.04 ha were established encompassing the structural variability of the area through the generated code (Tab. 1). Thus, LiDAR information was used in the sampling design process generating field sample plots which included the highest percentage of structural variability in the domain.

All plot locations were maintained at a proper distance from the roads and trails to avoid their possible effect (Fig. 1). In each 0.04 ha plot, we measured and identified all woody stems with diameter at breast height (DBH) ≥ 5 cm until the highest possible taxonomic level. The heights of all ferns and palms were measured with hypsometer Vertex III. All plots were located with a GPS Garmin GPSmap76Cx using the CRTM05 projection. This GPS device provides a typical Differential Global Positioning System horizontal accuracy lower than 5 meters.

Aboveground biomass for each tree (*agb*) inventoried in the plots was estimated using two different allometric models (Tab. 2). We used and compared the tropical wet forest stands allometric equations provided by Chave et al. (2005). In particular, model I was expressed as follows (eqn1):

$$agb = \exp\left[-2.557 + 0.940 \cdot \ln(\rho \cdot DBH^2 \cdot h)\right]$$

while model II had the following form (eqn. 2):

$$agb = \rho \cdot \exp[-1.239 + 1.98 \cdot \ln DBH + 0.207 \cdot (\ln DBH)^2 - 0.0281 (\ln DBH)^3]$$

where *agb* is the estimated individual tree oven-dry aboveground biomass (kg), *DBH* is the tree stem diameter at 1.3m (cm), *h* is the tree height (m) and ρ is the wood specific gravity (oven-dry wood over green volume, g cm^{-3}).

Measuring tree height is a hard task in this type of forest, so we used a combination of LiDAR measurements and diameter-based estimation to develop a height-diameter model. The maximum LiDAR height was related through a power regression with the maximum field measured diameter in each sample plot, in order to avoid unrealistic tree height estimates (Asner et al. 2013). This regression was applied to estimate each tree height.

Palms biomass was estimated using the equation (eqn. 3) proposed by Frangi & Lugo (1985) for the moist forests of Puerto Rico of *Prestoea montana (Graham) G. Nicholson*. The equation (eqn. 4) proposed by Tiepolo et al. (2002) for the *Cyathea* genus of tropical montane moist forests of Serra do Mar National Park, Brazil was used to estimate a ferns biomass (eqn. 3, eqn. 4):

$$agb = 10.0 + 6.4 \cdot h$$

$$agb = -\frac{4266348}{1 - 2792284 \cdot e^{0.313677 \cdot h}}$$

where *agb* is the estimated oven-dry aboveground biomass (kg) and *h* is the height (m) in both equations.

To estimate each tree wood specific gravity, we followed the Global Wood Density Database (Chave et al. 2009, Zanne et al. 2009). When it was not possible to use a value for a particular species, an average value at genus or family level was used. The 2008 Readiness Preparation Proposal (MINAET/FONAFIFO 2010) average values of wood density were applied when it was not possible to assign species, genus or family to the measured trees. These values are based on the research of Chudnoff cit. Solórzano (1992).

Aboveground biomass (*AGB*) of each field plot is the sum of the oven-dry aboveground biomass of all individual trees (*agb*), palms and ferns in the plot, expressed per hectare (Tab. 3).

Plot-aggregate allometry

We calculated for each sample plot the top-of-canopy height (TCH) (Asner & Mascaro 2014) which is considered as the average height of all 1 m resolution pixels of the Digital Canopy Model inside sample plots.

Tropical tree crowns can reach over 20 m in diameter; therefore, large probabilities exist for tree crowns to overlap adjacent 20×20 m plots. This limitation of the available field data may affect the results of the survey, so we increased cell size for processing LIDAR data to 25×25 m. In addition, by increasing cell size it is possible to minimize errors due to low GPS location accuracy, thus improving overlap between DCM cells and sample plots and ensuring that measured trees are taken into account in the remote sensing analysis.

Asner et al. (2011) proposed a plot-aggregate allometry inspired by the general tree allometric theory of Chave et al. (2005), which assumes that biomass follows the equation (eqn. 5):

$$agb = a \cdot DBH^{b1} \cdot h^{b2} \cdot \rho^{b3}$$

where *agb* is individual tree aboveground biomass, *DBH* is stem diameter (cm), *h* is canopy height (m), ρ is wood specific gravity (wood density, g cm^{-3}) and *a, b1, b2* and *b3* are the model parameters.

On the basis of this model, Asner & Mas-

Tab. 1 - Parameters measured in each 20×20 pixel to generate a code characterizing the vegetation structure of Poás National Park (Costa Rica).

Variable	Range	Value
Canopy cover	0-85.5 %	1
	85.5-99.5 %	2
	99.5-100 %	3
P95	2-21 m	1
	21-27 m	2
	>27 m	3
IQ	0-5 m	1
	5-8 m	2
	>8 m	3

Tab. 2 - Tree allometric equations used for aboveground biomass estimates in Poás Volcano National Park (Costa Rica). (nd): not determined.

Equation	DBH range (cm)	Number of individuals	R^2
Chave et al. (model I)	≥5 - 133.2	419	nd
Chave et al. (model II)	≥5 - 133.2	419	nd
Frangi & Lugo	-	25	0.96
Tiepolo et al.	-	22	0.88

Tab. 3 - Summary of the field plot parameters (n = 25) for aboveground biomass modeling in Poás Volcano National Park (Costa Rica). *AGB* has been calculated using two different tree-allometric equations from Chave et al. (2005)

Parameters	Mean	Minimum	Maximum	Standard Deviation
BA (m^2 ha^{-1})	58.50	30.97	84.11	13.04
Wood density (g cm^{-3})	0.60	0.51	0.70	0.05
Stem number (stems ha^{-1})	1699.00	425.00	2500.00	546.94
TCH (m)	15.28	8.51	20.74	3.34
AGB Chave's model I (t ha^{-1})	312.42	133.76	580.32	104.62
AGB Chave's model II (t ha^{-1})	405.16	168.26	987.69	175.10

caro (2014) fitted a general model of plot-aggregate aboveground biomass using a LiDAR plot network of tropical forest sites in Colombia, Hawaii, Madagascar, Peru and Panama to evaluate carbon density across a wide range of tropical vegetation conditions (eqn. 6):

$$AGB = 7.9912 \cdot TCH^{0.2807} \cdot BA^{0.9721} \cdot \rho_{BA}^{1.3763}$$

where *AGB* is the total plot aboveground biomass (t ha^{-1}), *TCH* is LiDAR-derived top-of-canopy height (m), *BA* is plot-averaged basal area (m^2 ha^{-1}) and ρ_{BA} is basal-area weighted wood density (g cm^{-3}). The general model was originally fitted to estimate aboveground carbon density. A factor of 0.48^{-1} (Martin & Thomas 2011) was used to convert aboveground carbon density model into aboveground biomass.

This method reduces the need for exhaustive plot-based inventories (Asner & Mascaro 2014) by relating *TCH* with *BA*, and *TCH* with wood density at regional level. Thus, *BA* is the only variable to be measured during the inventory, since density is considered as an average constant value for the plot.

We validated the general Asner & Mascaro's plot-aggregate allometry equation in our study area and we also fitted two specific models for the Poás Volcano forest following the same structure, one model using *AGB* estimations from Chave's equations I and the other one using *AGB* estimations from Chave's equation II. In order to fit the power *AGB* models we used the Nonlinear Least Squares (*nls*) function from the "stats" package included in the R software (R Core Team 2013). This function determines the nonlinear (weighted) least-squares estimate of the parameters of a nonlinear model using a Gauss-Newton algorithm.

Asner & Mascaro (2014) proposed a simple linear model forced through the origin to capture the *BA* variation in each region. This BA-TCH origin forced regression assumes that with a *TCH* of zero, *BA* must not be greater than zero. This ratio between *BA* and *TCH* is called a stocking coefficient (*SC* - Asner et al. 2012b) and explains structural variability across different tropical forests. In our study area, *SC* was estimated using a similar origin forced linear model.

Bias (*b*), root mean squared error (*RMSE*), relative bias (*b%*) and relative mean squared error (*RMSE%*) were calculated as principal contrasting statistics in the fitting phase of the *AGB* local model and in the validation of the general model in our study area (eqn. 7, eqn. 8, eqn. 9, eqn. 10):

$$b = \frac{\sum_{i=1}^{n} AGB_i - \widehat{AGB}_i}{n}$$

$$RMSE = \sqrt{\frac{\sum_{i=1}^{n} (AGB_i - \widehat{AGB}_i)^2}{n}}$$

$$b\% = \frac{b}{\overline{AGB}} \cdot 100$$

$$RMSE\% = \frac{RMSE}{\overline{AGB}} \cdot 100$$

where AGB_i is the true or reference aboveground biomass measured in field plots, $\widehat{AGB}_i$ is the aboveground biomass estimated by the model, *n* is the number of plots and $\overline{AGB}$ is the mean of the *AGB* field plot sample.

We mapped *AGB* across the landscape with LiDAR metrics using resolution of 25× 25 m, *i.e.*, each grid cell had the same area as cells used for LiDAR metrics processing, as other authors have already indicated (Magnussen & Boudewyn 1998). Top-of-canopy height, basal area and basal area weighted wood density were estimated in each cell. We then applied to each grid cell the general model and the two Poás forest models specifically fitted for this area.

Results and discussion

Field measured biomass

AGB for each plot was calculated using two different Chave's equations (eqn. 1 and eqn. 2). In order to use eqn. 1, single tree heights obtained through the height-diameter model were computed (eqn. 11)

$$h = 4.0197 \cdot DBH^{0.3814}$$

(R^2 = 0.49, RMSE = 3.97 m – see Fig. S1 in Supplementary material) where *h* is total tree height (m) and *DBH* is stem diameter (cm).

Aboveground biomass values (average ± standard deviation) estimated from the 25 field plots were 312.42 ± 104.62 t ha^{-1} when Chave's model I (eqn. 1) was used and 405.16 ± 175.1 with Chave's model II (eqn. 2). Mean basal area resulted in a value of 58.50 ± 13.04 m^2 ha^{-1} and average estimated wood density was 0.60 ± 0.05 g cm^{-3} (Tab. 3).

We observed important differences in the estimation of *AGB* (92.74 t ha^{-1} considering the mean value of plot sample) depending on the chosen tree allometry, affecting considerably and systematically the continuous estimation of *AGB* in the study area. Measuring heights of several dominant and intermediate trees with hypsometer in the plots could have improved this regression curve, though this option was not feasible during fieldwork due to time and budget constraints. Allometric errors, including systematic errors derived from the height-diameter model, might be the main cause of the differences when Chave's I and Chave's II models are used in the study area. Other authors have fixed the maximum LiDAR height to the maximum measured diameter for the same field plot to obtain a height-diameter model. This was considered as a conservative method to constrain their field-estimated carbon stocks for tropical dry forests and mangroves in Panama (Asner et al. 2013).

Plot-aggregate allometry

Basal area was related to *TCH* through the origin forced linear regression *BA-TCH* (Tab. 4). Both variables show significant correlation (p-value < 0.001). The stocking coefficient in our sampling (*SC* = 3.70) is higher than those reported by Asner & Mascaro (2014) in other tropical areas (1.13-2.58). This situation shows that Poás forest has larger biomass density for the same *THC* than the rest of the forests studied by Asner & Mascaro (2014).

Asner & Mascaro (2014) suggests that the *SC* varies regionally, *e.g.*, Asner et al. (2013) used only one *AGB-TCH* model to estimate aboveground biomass throughout the Republic of Panama. Although in this work *SC* was estimated for the entire area, the results show that *SC* might have different trends in each life zone (Fig. 2). The low number of plots constrained the estimation of reliable *SC* for different Holdridge's life zones.

Through the general model, aboveground biomass was estimated using only the field *BA* measurements. Asner & Mascaro (2014) suggested that relascope methods may be appropriate for quick *BA* measurements in-field. However, this method requires the development of a methodology to estimate a reliable *TCH* in variable-radius inventories.

There was no significant correlation between basal area weighted wood density and *TCH* (R^2 = 0.0014 and p-value > 0.05). These results combined with the small deviation of basal area weighted wood density in sampling (0.60 ± 0.05) suggest that it is possible to use a wood density constant value for the entire study area.

In the fitting phase the local models obtained a RMSE of 30.33 t ha^{-1} and 32.80 t ha^{-1} and were generated following the same structure as the general model (Tab.

Tab. 4 - Stocking coefficient (*SC*), local and general *AGB* models used in the study area. The parameters for the general model are taken from Asner & Mascaro (2014), while parameters for the local models have been adjusted for this work.

Models	Units	*a*	*b1*	*b2*	*b3*	*SC*	RMSE
Local basal area model	m^2 ha^{-1}	-	-	-	-	3.7	15.62
General model (Asner&Mascaro)	t ha^{-1}	7.9912	0.2807	0.9721	1.3763	-	34.26
Local model (Chave's model I)	t ha^{-1}	1.82137	0.3299	1.17488	1.05626	-	30.33
Local model (Chave's model II)	t ha^{-1}	1.92262	0.30201	1.17260	0.59760	-	32.80

4). The independent variables were significant at the 0.05 level. However, the models were not as consistent as before when basal area estimations from *TCH* were incorporated in the local model (Fig. S2 in the Supplementary material). This indicates low fitting of *TCH* and *BA* in this area and therefore, larger plots and/or different fits per life zone are required.

The comparison of *AGB* field plots measurements using Chave's model I and Chave's model II with *AGB* estimations obtained using the general model by Asner & Mascaro (2014 – Tab. 5) shows a better performance when Chave's II is used (Fig. 3), even though both models produce systematic deviations.

The general model was validated by the field plots measured data (*BA* and *BA*-weighted wood density) and by the estimated variables (predicted *BA* from *SC* and predicted mean weighted wood density – Tab. 5). Using Chave's equation II, the general model had low bias when *SC* was applied (*b* = -27.5 t ha^{-1}, *b%* = -6.79%). The large *RMSE* in the general model validation (more than 100 t^{-1}) was likely due to the small size plot. Small size plot generates large errors due to field sampling errors (Réjou-Méchain et al. 2014). In addition, small size plot increase the influence of edge effect and GPS errors in *TCH* and *AGB* field plot measurements. Mauya et al. (2015), working with *AGB* plot-level LiDAR models in northern Tanzania, reported that relative root mean square error decreased from 63.6 to 29.2% when the size plot was increased from 0.02 to 0.3 ha. We obtained a relative *RMSE* similar to that of Mauya et al. (2015) for similar plot size (0.04 ha).

Differences between field plots size and cell size for processing LiDAR data can be considered as an error source. Working with a large scale global data set, Réjou-Méchain et al. (2014) simulated the field sampling errors derived from the utilization of different sizes in field plots and remote sensing footprint. They showed that when field plots were very small (0.1 ha and below), the sampling error was mostly due to the contribution from field sampling, and was relatively insensitive to footprint area. According to that, we expect that *AGB* errors in Poás forest are more likely influenced by the small size of field plots than by the differences between the field plots size and the cell size for processing LiDAR data.

Our plot size (0.04 ha) was smaller than the one used for generating the general model (0.1-1.0 ha). Using small plots for estimating *AGB* or *BA* may result in improper estimations (Meyer et al. 2013, Mauya et al. 2015). Optimizing plot size is likely to be dependent not on plot size *per se*, but on the ratio of typical crown sizes to the plot size (Asner & Mascaro 2014). Three important outcomes are achieved using larger plots (> 0.5 ha): (1) the accuracy of plot-level biomass allometry improves as the number of trees increases (Asner &

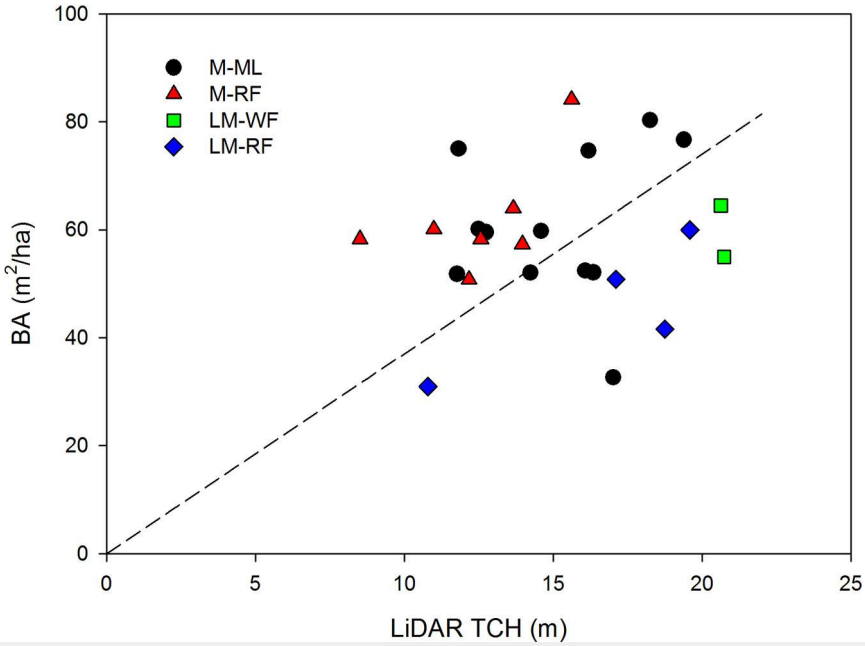

Fig. 2 - Relationship between LiDAR top of canopy heights (*TCH*) and basal area (stocking coefficient, *SC*) in each Holdridge's life zone of the Poás Volcano National Park (Costa Rica).

Tab. 5 - Comparison of the results obtained by the Asner & Mascaro's general model with the Chave's model I and model II and field measured basal area value (FM) or the stocking coefficient basal area value (*SC*). *b* is the bias, *RMSE* is the root mean squared error, *b%* is the relative bias and *RMSE%* is the relative mean squared error.

agb model	*BA*	*b*	*RMSE*	*b%*	*RMSE%*
Chave's model I	FM	-130.56	137.29	-41.79	43.94
Chave's model I	SC	-120.24	166.83	-38.49	53.40
Chave's model II	FM	-37.82	102.27	-9.33	25.24
Chave's model II	SC	-27.50	164.62	-6.79	40.63

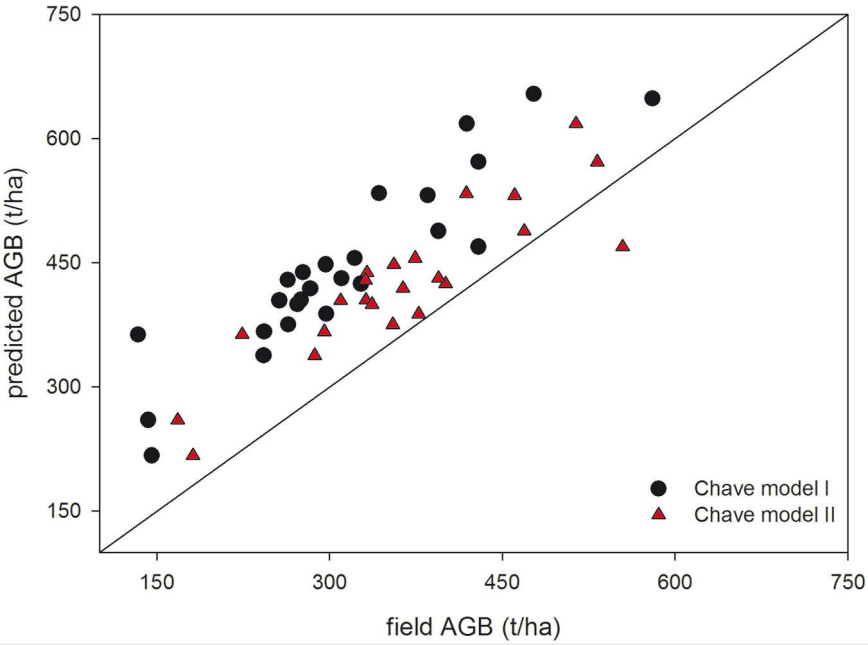

Fig. 3 - Estimated values of aboveground biomass using LiDAR derived data and the general approach (Asner & Mascaro 2014) against estimated aboveground values using field measurements and tree allometric equations of Chave's model I and model II in Poás Volcano National Park (Costa Rica).

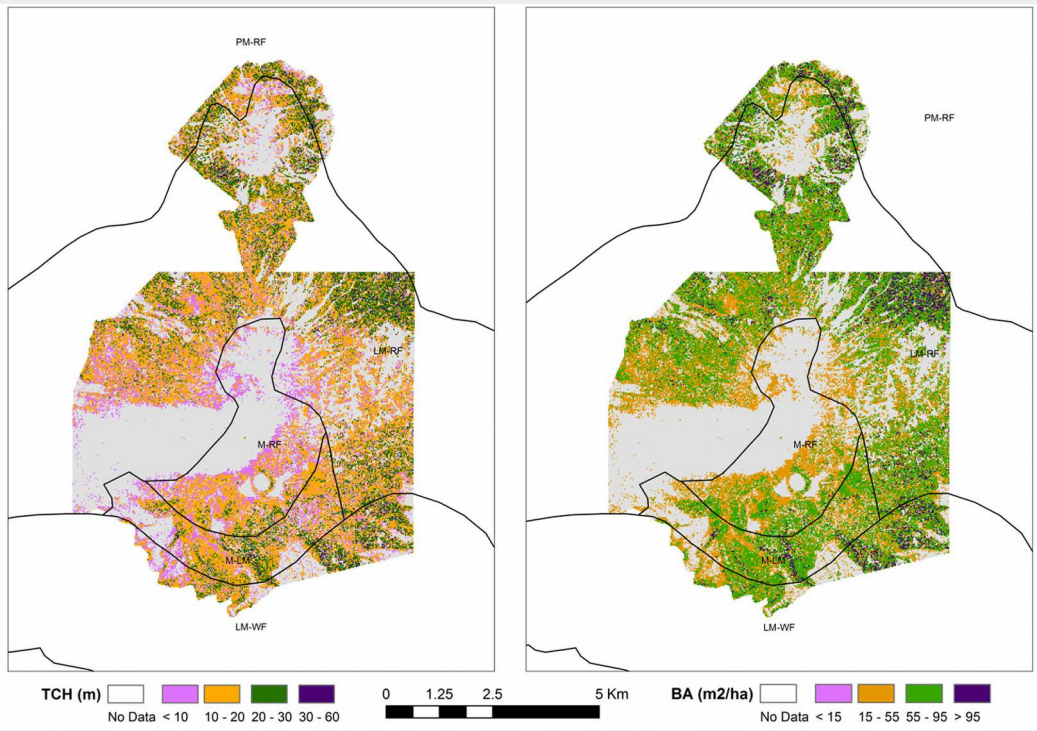

Fig. 4 – Top-of-canopy Height (*TCH*) and Basal Area (*BA*) values for Poás Volcano National Park (Costa Rica). *TCH* values were obtained through LiDAR data and *BA* values were derived from an origin-forced linear regression *BA-TCH*.

Mascaro 2014); (2) larger plots minimize the negative effect produced by low location accuracy due to GPS; (3) as tree crowns can exceed 20 m in diameter, it is possible that a tree crown studied in LiDAR data may not be part of a tree within the sample plot, leading to the so-called "edge effect". These three effects could be minimized by increasing plot size (Meyer et al. 2013), though leading to higher inventory costs. Additionally, size plots close to 1 ha could also be appropriate, as recent studies in tropical forests demonstrated that uncertainties approach 10% when plot sizes increase up to 1 ha (Asner & Mascaro 2014, Zolkos et al. 2013).

Plot-aggregate *AGB* models have biological meaning since main biomass factors are involved, *i.e.*, height, diameter (through basal area) and wood gravity. Height and diameter determine the tri-dimensional structure of forests and wood gravity details the stored carbon per unit volume.

In these types of forests large tree crowns in overstorey layers leads to an increase of first returns from the upper level of canopy recorded by the LiDAR system, overlooking the lower strata (Ediriweera et al. 2014). In this respect, *TCH* has broadly proved to be a good predictor of

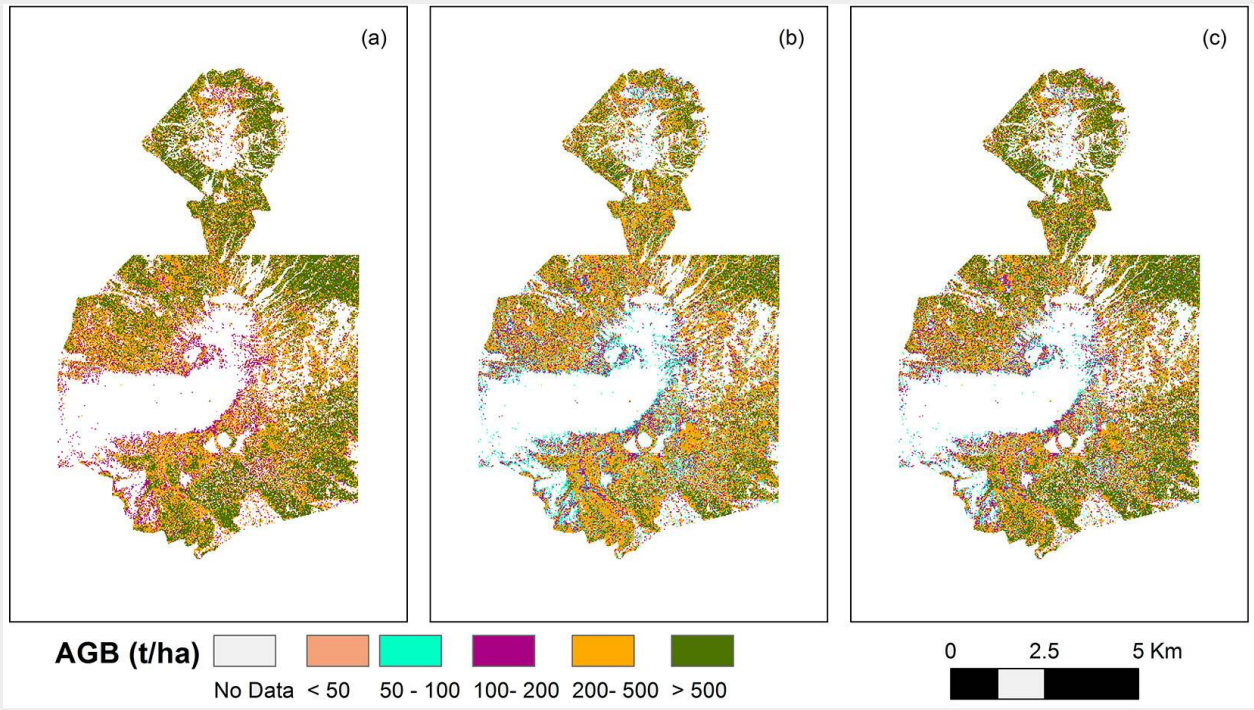

Fig. 5 - Distribution of estimated *AGB* (t ha^{-1}) in the study area of Poás Volcano National Park (Costa Rica). *AGB* was estimated by: (a) the general model (Asner & Mascaro 2014); (b) the local model using Chave's model I; and (c) the local model using Chave's model II.

forest structure, carbon density and biomass in tropical vegetation (Asner & Mascaro 2014).

Mapping biomass

Basal area values for the entire National Park were derived from the origin forced linear regression *BA-TCH* (Fig. 4). We used three *AGB* models (the general model and the two local fitted models) in order to map the *AGB* throughout the Holdridge's life zones in the study area (Fig. 5). We did not take into account cells with *TCH* under 4.5 m for a real comparison of stored biomass in each Holdridge's life zone, because of the extension of bare and shrub land, especially in the vicinity of crater areas and the bare eroded areas by lava streams.

The implementation of both locals and general models resulted in consistent and logical maps that showed no big differences between neighbor cells and yielded biomass values within the expected range for this type of forests (Fig. 5). The important differences observed in the estimation of *AGB* depending on the chosen tree allometry affects systematically to *AGB* mapping in the study area (Fig. 5). The total amount of *AGB* for the study area is considerably larger in the case of using local model I or the general model than using local model II. This points out the importance of individual tree biomass allometry in wall-to-wall aboveground biomass mapping.

Some authors have indicated the importance of the equivalence between the size of field plots and the size of pixel LiDAR processing (Magnussen & Boudewyn 1998). We have utilized the same size for the *TCH* computation in the field plots and in the whole area (25×25 m). This size is slightly smaller than the 30×30 m resolution used by Clark et al. (2011) or the 33×33 m used by Asner et al. (2009), simulating a typical biomass sample plot used in many tropical forests studies (Phillips et al. 1998).

Average values of 461.54 t ha^{-1}, 409.35 t ha^{-1} and 336.08 t ha^{-1}of *AGB* were determined for forest areas of Poás Volcano when general model, local model II and local model I were used, respectively. There are significant differences in total *AGB* in the study area depending on the applied model. The general model provided higher *AGB* than the local models, 11% higher than using local model II and 27% higher than local model I. Tree allometry is the main factor to explain these differences. Asner & Mascaro (2014) prioritized tree-level allometries based on local information, and measured tree height at least for the three largest trees in each plot, estimating the remaining tree heights using height-diameter allometry at the species or regional level. The general model was elaborated using a more adequate local tree allometry to each particular case, instead of the one used in this work. Therefore, the results derived from the general model are more likely adjusted to reality. The elaboration of local allometry models is an expensive process; thus, the general model is an adequate alternative when LiDAR data but not local tree-allometry are available in a specific area.

In all cases, the highest mean *AGB* value among life zones corresponded to premontane wet forest, situated at lower altitude, while the lowest value was achieved in the highest areas, *i.e.*, montane wet forest (Fig. 5). Thus, there is a biomass gradient with greater carbon stored in premontane wet forests, which are found at lower elevations where there is the highest rainfall (> 4000 mm y^{-1}) and located in the Pacific side of the Park (Fig. 5). This gradient has in the same trend reported by other tropical biomass studies (Girardin et al. 2010, Ulate 2010, Moser et al. 2011).

Conclusions

Allometry equations for the estimation of individual tree biomass are a critical factor to ensure wall-to-wall unbiased and accurate aboveground biomass mapping when plot-aggregate *AGB* local models are to be developed in new areas. *AGB* estimation can vary considerably depending on the tree allometric equations chosen or adjusted for a given study area. Differences between the results obtained with the general and the local models in our study area were significantly influenced by the applied tree allometry. The construction a local-specific allometry could improve the results, but it is more expensive. Therefore, a cost-benefit analysis might be carried out.

The alternative to developing specific tree allometry and local plot-aggregate models is the general plot-aggregate methodology, which can be easily and reliably applied. Aboveground biomass in a new study area could be estimated by measuring only the basal area (*BA*) in field plots in order to obtain a local *BA-TCH* regression. It presents an advantage over traditional intensive inventories for mapping biomass and carbon density in tropical forests, since local tree allometry and expensive time-consuming inventories are no longer required. It shows an easier approach to obtain *BA* through LiDAR top-of-canopy height (*TCH*) data, since *BA* is the only field measurement required. Therefore, the definition of precise *BA* field measurement procedures (*e.g.*, location, size and shape of the field plots) is decisive to achieve reliable results in future studies. We confirmed the influence of plot size on *BA-TCH* fittings; hence, an increment of plot size is recommended for future studies.

The results of this study show that the stocking coefficient (*SC*) may vary locally, even in small geographical areas (few thousand ha as the study area). More fieldwork is needed to demonstrate how *SC* varies between different life zones. The Poás Volcano National Park showed high values of *SC*, which implied that its forests exhibit a larger biomass density for the same *THC* compared to the rest of the forests studied by Asner & Mascaro (2014). Average basal area (58.50 ± 13.04 m^2 ha^{-1}) in the Poás Volcano National Park is significantly higher than in other forests. This parameter has a major influence on biomass storage, suggesting that these forests might play an important role as carbon sinks. In this sense, their protection and conservation is essential in a country devoted to a carbon neutral goal.

Acknowledgements

This work received a travel grant from the Technical University of Madrid. Poás Volcano National Park provided assistance, transport and lodging for the fieldworks. Authors thank Dr. Javier Bonatti (University of Costa Rica) for support, data access and sharing instruments for fieldwork.

References

Asner GP, Hughes RF, Varga TA, Knapp DE, Kennedy-Bowdoin T (2009). Environmental and biotic controls over aboveground biomass throughout a tropical rain forest. Ecosystems 12 (2): 261-278. - doi: 10.1007/s10021-008-9221-5

Asner GP, Hughes RF, Mascaro J, Uowolo AL, Knapp DE, Jacobson J, Kennedy-Bowdoin T, Clark JK (2011). High-resolution carbon mapping on the million hectare Island of Hawaii. Frontiers in Ecology and the Environment 9 (8): 434-439. - doi: 10.1890/100179

Asner GP, Mascaro J, Muller-Landau HC, Vieilledent G, Vaudry R, Rasamoelina M, Van Breugel M (2012a). A universal airborne LiDAR approach for tropical forest carbon mapping. Oecologia 168 (4): 1147-1160. - doi: 10.1007/s00442-011-2165-z

Asner GP, Clark JK, Mascaro J, García GA, Chadwick KD, Encinales DA, Paez-Acosta G, Cabrera E, Kennedy-Bowdoin T, Duque A, Balaji A, Von Hildebrand P, Maatoug L, Phillips JF, Knapp DE, Dávila MC, Jacobson J, Ordóñez MF (2012b). High-resolution mapping of forest carbon stocks in the Colombian Amazon. Biogeosciences Discussions 9 (3): 2683-2696. - doi: 10.5194/bg-9-2683-2012

Asner GP, Mascaro J, Anderson C, Knapp DE, Martin RE, Kennedy-Bowdoin T, Van Breugel M, Davies S, Hall JS, Muller-Landau HC, Potvi C, Sousa W, Wright J, Bermingham E (2013). High-fidelity national carbon mapping for resource management and REDD+. Carbon balance and management 8 (1): 1-14. - doi: 10.1186/1750-0680-8-7

Asner GP, Mascaro J (2014). Mapping tropical forest carbon: calibrating plot estimates to a simple LiDAR metric. Remote Sensing of Environment 140: 614-624. - doi: 10.1016/j.rse.2013.09.023

Bolaños R, Watson V, Tosi J (2005). Mapa ecológico de Costa Rica (Zonas de Vida), según el sistema de clasificación de zonas de vida del mundo de L.R. Holdridge), Escala 1: 750 000. [Ecological map of Costa Rica (Life Zones) according to the classification system of Holdridge life zones in the world, Scale 1:750.000]. Centro Científico Tropical, San José, Costa Rica. [in Spanish]

Bonan GB (2008). Forests and climate change:

forcings, feedbacks, and the climate benefits of forests. Science 320 (5882): 1444-1449. - doi: 10.1126/science.1155121
Chave J, Andalo C, Brown S, Cairns MA, Chambers JQ, Eamus D, Fölster H, Fromard F, Higuchi N, Kira T, Lescure JP, Nelson BW, Ogawa H, Puig H, Riéra B, Yamakura T (2005). Tree allometry and improved estimation of carbon stocks and balance in tropical forests. Oecologia 145 (1): 87-99. - doi: 10.1007/s00442-005-0100-x
Chave J, Coomes DA, Jansen S, Lewis SL, Swenson NG, Zanne AE (2009). Towards a worldwide wood economics spectrum. Ecology Letters 12 (4): 351-366. - doi: 10.1111/j.1461-0248.2009.01285.x
Clark ML, Clark DB, Roberts DA (2004). Small-footprint lidar estimation of sub-canopy elevation and tree height in a tropical rain forest landscape. Remote Sensing of Environment 91 (1): 68-89. - doi: 10.1016/j.rse.2004.02.008
Clark ML, Roberts DA, Ewel JJ, Clark DB (2011). Estimation of tropical rain forest aboveground biomass with small-footprint lidar and hyperspectral sensors. Remote Sensing of Environment 115 (11): 2931-2942. - doi: 10.1016/j.rse.2010.08.029
Ediriweera S, Pathirana S, Danaher T, Nichols D (2014). LiDAR remote sensing of structural properties of subtropical rainforest and eucalypt forest in complex terrain in North-eastern Australia. Journal of Tropical Forest Science 26 (3): 397-408. [online] URL: http://www.jstor.org/stable/43150922
Frangi JL, Lugo AE (1985). Ecosystem dynamics of a subtropical floodplain forest. Ecological Monographs 55 (3): 351-369. - doi: 10.2307/1942582
Gibbs HK, Brown S, Niles JO, Foley JA (2007). Monitoring and estimating tropical forest carbon stocks: making REDD a reality. Environmental Research Letters 2 (4): 045023. - doi: 10.1088/1748-9326/2/4/045023
Girardin CAJ, Malhi Y, Aragao LEOC, Mamani M, Huaraca Huasco W, Durand L, Feeley KJ, Rapp J, Silva-Espejo JE, Silman M, Salinas N, Whittaker RJ (2010). Net primary productivity allocation and cycling of carbon along a tropical forest elevational transect in the Peruvian Andes. Global Change Biology 16 (12): 3176-3192. - doi: 10.1111/j.1365-2486.2010.02235.x
Houghton RA (2005). Tropical deforestation as a source of greenhouse gas emissions. In: "Tropical deforestation and climate change" (Moutinho P, Schwartzman S eds). Instituto de Pesquisa Ambiental da Amazônia and Environmental Defense Fund, Belém, Pará, Brazil, pp. 13-22. [online] URL: http://rainforestcoalition.org.serv7.temphostspace.com/documents/Tropicaldeforestationandclimatechange.pdf#page=13
IPCC (2005). Orientación sobre las buenas prácticas para uso de la tierra, cambio de uso de la tierra y silvicultura [Good practices guidance on land use, land use change and silviculture]. Programa del IPCC sobre inventarios nacionales de gases de efecto invernadero. IPCC, Geneve, Switzerland, pp. 628. [In Spanish]
IPCC (2007). Contribution of Working Groups I, II and III to the Fourth Assessment Report of the Intergovernmental Panel on Climate Change: Synthesis Report (Pachauri RK, Reisinger A eds). IPCC, Geneva, Switzerland, pp. 104.
Magnussen S, Boudewyn P (1998). Derivations of stand heights from airborne laser scanner data with canopy-based quantile estimators. Canadian Journal of Forest Research 28 (7): 1016-1031. - doi: 10.1139/x98-078
Martin AR, Thomas SC (2011). A reassessment of carbon content in tropical trees. PLoS ONE 6 (8): e23533. - doi: 10.1371/journal.pone.0023533
Mauya EW, Hansen EH, Gobakken T, Bollandsas OM, Malimbwi RE, Naesset E (2015). Effects of field plot size on prediction accuracy of aboveground biomass in airborne laser scanning-assisted inventories in tropical rain forests of Tanzania. Carbon Balance and Management 10 (1): 1003. - doi: 10.1186/s13021-015-0021-x
Meyer V, Saatchi SS, Chave J, Dalling JW, Bohlman S, Fricker GA, Robinson C, Neumann M, Hubbell S (2013). Detecting tropical forest biomass dynamics from repeated airborne Lidar measurements. Biogeosciences 10 (8): 5421-5438. - doi: 10.5194/bg-10-5421-2013
MINAET/FONAFIFO (2010). Propuesta para la preparación de readiness R-PP Costa Rica [Costa Rica readiness preparation proposal]. Forest Carbon Partnership Facility, Ministerio de Ambiente, Energía y Telecomunicaciones (MINAET), Fondo Financiación Forestal (FONAFIFO), San José, Costa Rica, pp. 150. [In Spanish]
Mitchard ETA, Saatchi SS, White LJT, Abernethy KA, Jeffery KJ, Lewis SL, Collins M, Lefsky MA, Leal ME, Woodhouse IH, Meir P (2012). Mapping tropical forest biomass with radar and spaceborne LiDAR: overcoming problems of high biomass and persistent cloud. Biogeosciences Discussions 8 (4): 8781-8815. - doi: 10.5194/bgd-8-8781-2011
Moser G, Leuschner C, Hertel D, Graefe S, Soethe N, Iost S (2011). Elevation effects on the carbon budget of tropical mountain forests (S Ecuador): the role of the belowground compartment. Global Change Biology 17 (6): 2211-2226. - doi: 10.1111/j.1365-2486.2010.02367.x
Murdiyarso D, Skutsch M, Guariguata M, Kanninen M, Luttrell C, Verweij P, Stella O (2008). Measuring and monitoring forest degradation for REDD: implications of country circumstances. Tijdschrift: tijdelijk onbekend 16. [online] URL: http://dspace.library.uu.nl/handle/1874/32927
Phillips OL, Mahli Y, Higuchi N, Laurance WF, Nuñez PV, Vázquez RM, Laurance SG, Fereira LV, Stern M, Brown S, Grace J (1998). Changes in the carbon balance of tropical forests: evidence from long-term plots. Science 282: 439-42. - doi: 10.1126/science.282.5388.439
Pirotti F (2011). Analysis of full-waveform LiDAR data for forestry applications: a review of investigations and methods. iForest - Biogeosciences and Forestry 4 (3): 100-106. - doi: 10.3832/ifor0562-004
R Core Team (2013). R: a language and environment for statistical computing. R Foundation for Statistical Computing. Vienna, Austria. [online] URL: http://www.R-project.org/
Réjou-Méchain M, Muller-Landau HC, Detto M, Thomas SC, Toan TL, Saatchi SS, Brockelman WY (2014). Local spatial structure of forest biomass and its consequences for remote sensing of carbon stocks. Biogeosciences Discussions 11: 5711. [online] URL: http://scholarworks.umt.edu/forest_pubs/47/
Sasaki N, Putz FE (2009). Critical need for new definitions of "forest" and "forest degradation" in global climate change agreements. Conservation Letters 2: 226-232. - doi: 10.1111/j.1755-263X.2009.00067.x
Sexton JO, Bax T, Siqueira P, Swenson JJ, Hensley S (2009). A comparison of lidar, radar, and field measurements of canopy height in pine and hardwood forests of southeastern North America. Forest Ecology and Management 257 (3): 1136-1147. - doi: 10.1016/j.foreco.2008.11.022
Simonian L, Hernández Munguía JG, Arana Noguera GA, Thomas L, Middleton J, Phillips A (2010). Global forest resources assessment 2010: main report (No. FAO FP-163). FAO, Rome, Italy, pp. 340.
Solórzano X (1992). La depreciación de los recursos naturales en Costa Rica y su relación con el Sistema de Cuentas Nacionales [Depreciation of Natural Resources in Costa Rica and its relationship with the System of National Accounts]. World Resources Institute (WRI), Centro Científico Tropical (CCT), San José, Costa Rica, pp. 152. [in Spanish]
Tiepolo G, Calmon M, Feretti AR (2002). Measuring and monitoring carbon stocks at the Guaraquecaba climate action project, Parana, Brazil. In: Proceedings of the "International Symposium on Forest Carbon Sequestration and Monitoring" (Taiwan Forestry Research ed). Taipei (Taiwan) 11-15 Nov 2002, pp. 98-115.
Ulate CA (2010). Análisis y comparación de la biomasa aérea de la cobertura forestal según zona de vida y tipo de bosque para Costa Rica [Analysis and comparison of aboveground biomass in different living areas and forest types in Costa Rica]. Instituto Tecnológico de Costa Rica, Escuela de Ingeniería Forestal, Cartago, Costa Rica, pp. 60. [in Spanish]
Zanne AE, Lopez-Gonzalez G, Coomes DA, Ilic J, Jansen S, Lewis SL, Miller RB, Swenson NG, Wiemann MC, Chave J (2009). Data from: Towards a worldwide wood economics spectrum. Dryad Digital Repository. - doi: 10.5061/dryad.234
Zolkos SG, Goetz SJ, Dubayah R (2013). A meta-analysis of terrestrial aboveground biomass estimation using LiDAR remote sensing. Remote Sensing of Environment 128: 289-298. - doi: 10.1016/j.rse.2012.10.017

Supplementary Material

Fig. S1 - Correlation between LiDAR maximum plot heights (m) and maximum diameter measured at field plots in Poás National Park (Costa Rica).

Fig. S2 - Fitting local Poás model with TCH-derived basal area (a) resulted in greater deviations than fitting with field measured basal area (b).

Link: Fernandez-Landa_1744@suppl001.pdf